The Canadian Mineralogist
Vol. 44, pp. 1499-1512 (2006)

THE CRYSTAL STRUCTURE OF DADSONITE

EMIL MAKOVICKY[§]

Geological Institute, University of Copenhagen, Østervoldgade 10, DK–1350 Copenhagen K, Denmark

DAN TOPA

Department of Material Science, University of Salzburg, Hellbrunnerstr. 34, A–5020 Salzburg, Austria

WILLIAM G. MUMME

CSIRO Minerals, Bayview Avenue, Clayton 3168, Australia

ABSTRACT

The crystal structure of dadsonite, ideally $Pb_{23}Sb_{25}S_{60}Cl$, *a* 8.276(2), *b* 17.392(4), *c* 19.505(4) Å, α 83.527(7), β 77.882(8), γ 89.125(8)°, *V* 2727.2(9), space group $P\bar{1}$ and $Z = 1$, from the Klačianka hydrothermal deposit, in the Low Tatra Mountains of Slovakia, has been refined to an R_1 index of 4.90% for 5263 unique reflections [$F_o^2 \geq 2\sigma(F^2)$] measured with Mo$K\alpha$ radiation on a three-circle diffractometer equipped with a CCD detector. There are 10 pure Pb and 8 Sb sites, as well as three mixed (Pb,Sb) and (Sb,Pb) sites and three split coordinations of Sb in the crystal structure. Thirty S positions and one presumed Cl position, designated as "S1", constitute the anion part of the structure. The structure is of a rod-layer type, with two types of rod-layers alternating along the stacking direction *b*. Dadsonite is a desymmetrized OD structure with profuse twinning. The two types of layers present possess layer symmetries $p\bar{1}$ and $b2/m11$, respectively. These layers respectively have a pseudoperiodicity equal to *a*/2 and a set of elements of pseudosymmetry which together cause a disorder process.

Keywords: dadsonite, Pb–Sb sulfosalt, crystal structure, chlorosulfide.

SOMMAIRE

Nous avons affiné la structure cristalline de la dadsonite, de composition idéale $Pb_{23}Sb_{25}S_{60}Cl$, *a* 8.276(2), *b* 17.392(4), *c* 19.505(4) Å, α 83.527(7), β 77.882(8), γ 89.125(8)°, *V* 2727.2(9) Å^3, groupe spatial $P\bar{1}$ et $Z = 1$, provenant du gisement hydrothermal de Klačianka, dans les montagnes bas Tatra de Slovaquie, jusqu'à un résidu R_1 de 4.90% en utilisant 5263 réflexions uniques [$F_o^2 \geq 2\sigma(F^2)$] mesurées avec rayonnement Mo$K\alpha$ sur un diffractomètre à trois cercles muni d'un détecteur de type CCD. La structure contient dix sites occupés entièrement par Pb et huit sites à Sb, ainsi que trois sites à occupation mixte (Pb,Sb) et (Sb,Pb), et trois sites ayant une coordinence partagée de Sb. Trente positions de S et une position présumée de Cl, désignée "S1", constituent la partie anionique de la structure. Cette structure, du type "bâtonnets en couches" , comporte deux sortes de ces agencements en alternance le long de la direction d'empilement *b*. La dadsonite aurait une structure OD dissymétrisée avec maclage répandu. Les deux sortes de couches ont une symétrie $p\bar{1}$ et $b2/m11$, respectivement. Ces couches possèdent à la fois une pseudopériodicité égale à *a*/2 et un ensemble d'éléments de pseudosymétrie qui ensemble causent un processus de désordre.

(Traduit par la Rédaction)

Mots-clés: dadsonite, sulfosel Pb–Sb, structure cristalline, chlorosulfure.

§ *E-mail address*: emilm@geol.ku.dk

Introduction

Dadsonite was defined by Jambor (1969) as a new sulfantimonite species from four distinct localities: Yellowknife in the Northwest Territories, and Madoc, Ontario, both in Canada, Pershing County, Nevada, U.S.A., and Wolfsberg, Germany. He determined the mineral to be monoclinic, with *a* 19.05 Å, *b* 4.11 Å, *c* 17.33 Å and β 96°20´, and established the chemical formula as $Pb_{11}Sb_{12}S_{29}$. A detailed chemical analysis and X-ray-diffraction studies of dadsonite from Saint-Pons, Alpes de Haute-Provence, France by Moëlo (1979) and Cervelle *et al*. (1979) established its composition as $Pb_{23}Sb_{25}ClS_{60}$, and confirmed its monoclinic symmetry [*a* 19.041(7) Å, *b* 8.226(3) Å, *c* 17.327(7) Å, β 96°18´, refined from powder data]. The crystal structure of the 4 Å subcell of dadsonite was determined by Makovicky & Mumme (1984) in space group *P*2/*m* and illustrated in Makovicky (1993, 1997). The poor quality of the acicular crystals from Saint-Pons did not allow a proper refinement of the structure.

Dadsonite is not just another lead–antimony sulfosalt. It has been described as one of the very few natural chlorosulfosalts, an interesting product of the reaction of highly chlorinated solutions with the older Pb–Sb sulfides and sulfosalts in hydrothermal deposits (Moëlo 1979). It is the least chlorinated member of a potential series of chlorinated sulfosalts, synthesized by Moëlo (1979), Bortnikov *et al.* (1979) and Kostov & Macíček (1995), and observed in nature by Breskovska *et al*. (1982) and Moëlo *et al*. (1989). Thus, the crystal structure of dadsonite is a good point of departure for a study of the crystal–chemical role of chlorine in Pb–Sb sulfosalts, and a new refinement on a better-quality material became desirable.

Chemical Composition

Quantitative chemical data for dadsonite from Klačianka, Low Tatra Mountains, in Slovakia, were obtained with an electron microprobe (JEOL Superprobe JXA–8600 operated at 25 kV and 35 nA, and controlled by the Advanced Microbeam, Probe for Windows system of programs), installed at the Department of Geography, Geology and Mineralogy, University of Salzburg. The following standards and X-ray lines were used: natural PbS (galena; Pb*L*α), Sb_2S_3 (stibnite; Sb*L*α, S*K*α), HgS (cinnabar; Hg*L*α), $CuFeS_2$ (chalcopyrite; Cu*K*α), synthetic Ag metal (Ag*L*α) and NaCl (Cl*K*α). The raw data were corrected with the on-line ZAF–4 procedure. The results, obtained from eight-point analyses on different grains, show only minor variation of the chemical composition of dadsonite, and a constant presence of Cl (Table 1). The chemical composition obtained conforms fully with the formula established by Moëlo *et al*. (1989).

TABLE 1. CHEMICAL COMPOSITION OF DADSONITE FROM THE LOW TATRA MOUNTAINS

Element	Pb	Sb	S	Cl	Total
wt.%	48.64	31.09	19.50	0.38	99.61
Std. dev.	0.30	0.14	0.09	0.03	0.40
Atomic ratios	22.99	25.01	59.57	1.04	
Std. dev.	0.08	0.13	0.14	0.08	

Average result of eight point-analyses. Atomic ratios were normalized to Σ(Pb + Sb) = 48 atoms.

X-Ray Crystallography

Several needle-like crystals, extracted from dadsonite aggregates, were investigated with a Bruker AXS diffractometer equipped with a CCD area-detector using graphite-monochromated Mo*K*α radiation. After many trials, a crystal suitable for structural investigation was found. Experimental settings are listed in Table 2. The Smart (Bruker AXS, 1998) system of programs was used for unit-cell determination and data collection, Saint+ (Bruker AXS, 1998) for the calculation of integrated intensities, and Xprep (Bruker AXS, 1998) for empirical absorption-corrections based on pseudo Ψ-scans. The centrosymmetric space-group $P\bar{1}$, proposed by the Xprep program, was chosen; it is consistent with the triclinic symmetry of the lattice and intensity statistics (mean $|E^2 - 1| = 1.259$). The structure of dadsonite was solved by direct methods (program Shelxs of Sheldrick 1997a), which revealed most of the cation positions. In subsequent cycles of the refinement (program Shelxl of Sheldrick 1997b), the positions of additional atoms were deduced from difference-Fourier syntheses. The structure obtained agrees in all principal features with that determined by Makovicky & Mumme (1984). Refinement data are given in Table 2, and the fractional coordinates and isotropic and anisotropic displacement parameters of all atoms are listed in Table 3. Selected *Me*–S bond distances are presented in Table 4, and selected geometrical parameters for individual coordination-polyhedra, calculated with the Ivton program (Balić-Žunić & Vicković 1996), are given in Table 5. A table of structure factors for dadsonite may be obtained from the Depository of Unpublished Data, CISTI, National Research Council, Ottawa, Ontario K1A 0S2, Canada.

The Overall Structural Scheme

The crystal structure of dadsonite consists of rods of an SnS-like arrangement, infinite along [001] of the SnS archetype. These rods, three coordination pyramids of Pb or Sb wide, and four combined sulfur-and-metal sheets thick, are organized into two alternating, distinct types of layers (Fig. 1), the so-called *rod-layers* of Makovicky (1993). Their inner portions are occupied by

square coordination pyramids of (primarily) Sb, which form the caps of the central row of "standing" trigonal coordination-prisms hosting the pairs of lone electrons of the Sb atoms. The outer surfaces consist of square coordination-pyramids of Pb, forming part of variously capped trigonal coordination-prisms of Pb.

The Pb prisms span the zig-zag interspaces between adjacent rod-layers. Inspection of these interspaces reveals that each straight interval in them represents a non-commensurate fit between the pseudotetragonal, Pb-rich surface (Q) of one rod and the pure-anion, sheared hexagonal $3^2 \bullet 4^2$ surface (H) of the opposing rod. The observed matches are 2 Q : 1½ H and 3 Q : 2 H in terms of surface submesh; they can be traced in Figure 1, where the noncommensurate interspaces were left uncolored.

The two rod-layers differ in the interconnection of the rods. One set of rod-layers, at $y = ½$ in Figure 1, have rods interconnected *via* a single row of anions, denoted S1 in Figure 2. These anions are underbonded, situated between the flanking rows of S atoms, all these anions forming the shared faces of two tricapped trigonal coordination prisms of lead. Therefore, the S1 site is the potential Cl site in the structure. This layer is the rod-layer of Type 5 of Makovicky (1993), also known from the structure of $Pb_{12.7}Sb_{11.4}S_{28.4}Cl_{2.7}$ (Kostov & Macíček 1995).

The other set of rod-layers (at $y = 0$) has adjacent rods interconnected *via* a pair of standing, monocapped coordination-prisms of antimony. In projection (Fig. 1), it resembles such an interconnection in the structure of cosalite, ~$Pb_2Bi_2S_5$ (Srikrishnan & Nowacki 1974). However, in cosalite, these elements are octahedra and not trigonal prisms, in agreement with the lesser steric activity of the pair of lone electrons on the Bi atoms. Thus, in the present layer (the Type-3_{SnS} layer of Makovicky 1997), the adjacent rows of Pb are on the same structural levels (although they do not share the same x coordinate because of the large β angle). This situation is unlike that in cosalite, where the corresponding rows are mutually displaced by 2 Å along the lattice direction that has the 4 Å periodicity.

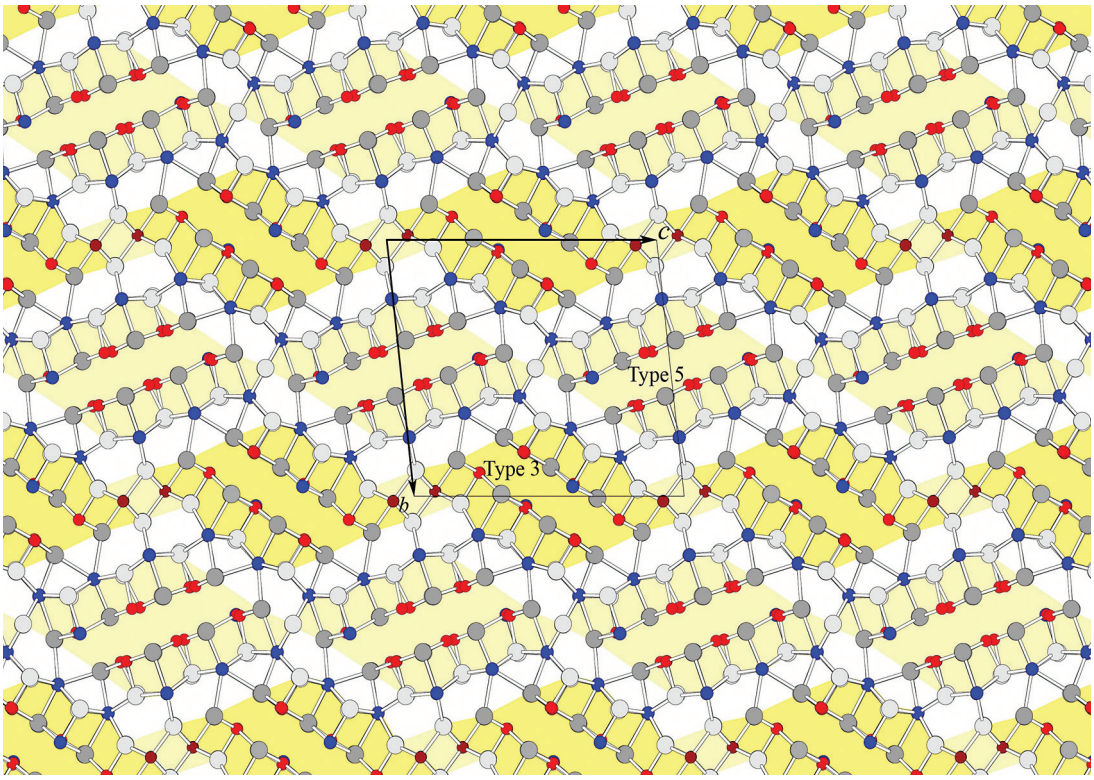

FIG. 1. Projection of the crystal structure of dadsonite along [100]. The *b* axis points downward, and the *c* axis is horizontal. In the order of decreasing size, spheres represent: sulfur (and chlorine) (white), lead (blue), and (predominantly) antimony (red). Light and dark spheres are strings of atoms mutually shifted along [100] by ~2 Å. Shading indicates rods constituting rod-layers (010) of two types, at $y = 0$ and $y = ½$, respectively.

TABLE 2. EXPERIMENTAL AND REFINEMENT DETAILS, SINGLE-CRYSTAL X-RAY-DIFFRACTION STUDY OF DADSONITE*

Crystal data		
Chemical formula, formula weight	$Pb_{11}Sb_{13}S_{30}Cl_{0.5}$	
Cell setting, Space group	triclinic, $P\bar{1}$	
a (Å)	8.276(2)	4.1382(9)
b (Å)	17.392(4)	17.394(4)
c (Å)	19.505(4)	19.071(4)
α (°)	83.527(7)	96.442(7)
β (°)	77.882(8)	90.113(8)
γ (°)	89.215(8)	90.775(7)
V (Å^3)	2727.2 (9)	1364.0(5)
Z	2	1
D_x (Mg m^{-3})	5.88	
No. of reflections for cell parameters	3691	3525
μ (mm^{-1})	40.97	
Crystal habit, color	needle, metallic	
Crystal size	0.10 × 0.03 × 0.02	
Data collection		
T_{min}, T_{max}	0.131, 0.459	
No. of measured reflections	19729	9658
No. of independent reflections	8710	4306
No. of observed reflections	5263	3531
Criterion for observed reflections	$I > 2\sigma(I)$	
R_{int} (%)	7.4	6.88
Range of h, k, l	$-9 \le h \le 9$ $-20 \le k \le 20$ $-23 \le l \le 22$	$-4 \le h \le 4$ $-20 \le k \le 20$ $-22 \le l \le 22$
Refinement		
Refinement on F_o^2		
R [$F_o > 4\sigma(F_o)$] (%)	4.90	4.94
wR (F_o^2)	12.12	12.86
S (*GooF*)	0.935	1.086
No. of reflections used in refinement	5263	3531
No. of parameters refined	489	246
Weighting scheme	a = 0.0413, b = 3.43	a = 0.0613, b = 3.28
	$w = 1/[\sigma_2(F_o^2) + (aP)^2 + bP]$, where $P = (F_o^2 + 2F_c^2) / 3$	
$(\Delta/\sigma)_{max}$	0.000	
$\Delta\rho_{max}$ (e/Å^3)	3.74 (0.97 Å from Pb11)	3.63 (0.79 Å from Sb1)
$\Delta\rho_{min}$ (e/Å^3)	–2.15 (1.01 Å from Pb7)	–2.13 (0.64 Å from S)
Extinction method	none	
Source of scattering factors	*International Tables for X-Ray Crystallography* (1992, Vol. C, Tables 4.2.6.8 and 6.1.1.4)	
Computer programs		
Structure solution	SHELXS97 (Sheldrick 1997a)	
Structure refinement	SHELXL97 (Sheldrick 1997b)	

* Data for 8 Å and 4Å refinements, respectively.

Detailed Structure of the Rods

The triple ribbons [100] of the square coordination-pyramids of antimony in the Type-3 layers (Fig. 3) consist of (a) the marginal site Sb1, followed by Sb13 along [100], (b) a similar pair Sb5 and Sb8 at the opposing margin of the ribbon, as well as (c) the central pair Sb3 and Sb10. The ribbons are polar, with short Sb–S bonds oriented in one way, on the side of +[100]. If the splitting of the Sb1 and S13 sites, and a partial substitution of Sb3 by lead, are ignored, these ribbons are similar to those in jamesonite (Niizeki & Buerger 1957). Across the *lone-electron-pair micelle* (*i.e.*, the common volume accommodating the lone-electron pairs of Sb) of the Type-3 rod, they are inversion-related with respect to the opposing Sb ribbon. These ribbons are backed by trigonal-prismatic Pb2, 5, 6, 7, 8, and 10 sites, as well as by Sb2 and Sb12.

Because of the approximate correspondence between Sb1 and Sb13, Sb5 and Sb8, Sb3 and Sb10, as well as Sb2 and Sb12, Pb5 and Pb8, and Pb2 and Pb12, the Type-3 layer has, to a good approximation, two repeat periods within one *a* period of the lattice. Also, the inversion centers occur with double density: the set of exact inversion-centers, relating the same atomic sites on the two sides of the lone-electron-pair micelles, alternates with another (approximate) set, relating the approximately identical sites (*e.g.,* Sb1 and Sb13, Sb5 and Sb8, *etc*.) on these two sides of the micelle. The implications of this arrangement will be given in the following section.

The Type-5 layer at $y = ½$ has a completely different configuration surrounding its central lone-electron-pair micelle (Fig. 3). The triple ribbon with marginal Sb4 and Sb9, central Sb6 and Sb7, and again marginal Sb11 and Pb4 sites (the latter pair represents a [100] column with mixed composition), consists of trapezoidally distorted "square" coordination-pyramids. In the [100] direction, the orientations of short Sb–S bonds in the pyramid bases alternate between, approximately, [012] and [$01\bar{2}$] directions. The $Sb7S_3$ and $Sb4S_3$ groups form a pair bridged *via* common S2 and S29 ligands, whereas the other Sb sites form solitary SbS_3 groups. Atom Sb6, with its two short Sb6–S25 and Sb6–S5 bonds, forces Pb4 into a trapezoidal and eccentric coordination (Fig. 3b).

There is no subperiod *a*/2 in this type of layer, but it has a set of (approximate) mirror planes (100)* through the Sb4–Sb11 sites and, again through the Sb9–Pb4 sites. Across the lone-electron-pair micelle, these triple ribbons are related by centers of symmetry situated on the atomic levels (those of Pb atoms in the surface of the layer) half-way between the local mirror planes of the rod. Approximate two-fold axes parallel to [100] pass through the S(Cl)1 position, and similar 2_1 axes pass through the centers of lone-electron-pair micelles.

Cation Polyhedra

There are two types of lead sites in dadsonite, (a) the mono- and the bicapped trigonal coordination prisms of Pb1–3 and Pb5–11 along the surface of structural rods, and (b) the Pb4, Pb12, and Pb13 sites substituting to various extents for the antimony in the triple ribbons of Sb coordination-pyramids (Figs. 2, 3a, b).

The monocapped "flat-lying" trigonal prisms of Pb3, Pb5, Pb8, and Pb9 (Figs. 1, 2) display an active lone-electron pair, so that the Pb–S distances across the interspace are the longest distances, of the order of 3.09–3.26 Å (Table 4). This situation is not expressed by

TABLE 3. POSITIONAL AND DISPLACEMENT PARAMETERS FOR THE 8 Å STRUCTURE OF DADSONITE

ATOM	*sof*	*x*	*y*	*z*	*U*eq	U_{11}	U_{22}	U_{33}	U_{23}	U_{13}	U_{12}
Pb1		0.01133(11)	0.76979(6)	0.00506(5)	0.0236(3)	0.0251(5)	0.0231(6)	0.0216(5)	0.0013(4)	-0.0045(4)	0.0038(3)
Pb2		0.09059(11)	0.84888(6)	0.77863(5)	0.0251(3)	0.0235(5)	0.0321(7)	0.0196(5)	-0.0076(5)	-0.0022(5)	-0.0026(5)
Pb3		0.10223(11)	0.32396(6)	0.78080(5)	0.0211(2)	0.0229(5)	0.0211(6)	0.0189(5)	-0.0033(4)	-0.0031(5)	0.0014(4)
Pb4	0.648(9)	0.1025(3)	0.4633(2)	0.2931(2)	0.0162(5)						
Sb14	0.352(9)	0.129(1)	0.4626(5)	0.2950(5)	0.0162(5)						
Pb5		0.18480(11)	0.73765(6)	0.60477(5)	0.0221(2)	0.0212(5)	0.0269(6)	0.0179(5)	-0.0041(4)	-0.0028(4)	0.0001(4)
Pb6		0.21059(11)	0.39080(6)	0.57004(5)	0.0268(3)	0.0240(6)	0.0333(7)	0.0237(5)	-0.0032(5)	-0.0066(4)	-0.0005(5)
Pb7		0.27458(11)	0.61319(6)	0.42895(5)	0.0264(3)	0.0238(6)	0.0331(7)	0.0231(5)	-0.0049(5)	-0.0058(4)	0.0011(5)
Pb8		0.32374(11)	0.26441(6)	0.39448(5)	0.0220(2)	0.0206(5)	0.0277(7)	0.0181(5)	-0.0041(4)	-0.0040(4)	0.0014(4)
Pb9		0.39622(11)	0.67579(6)	0.21894(5)	0.0209(2)	0.0232(5)	0.0214(6)	0.0185(5)	-0.0031(4)	-0.0051(4)	0.0016(4)
Pb10		0.41029(11)	0.15288(6)	0.22049(5)	0.0234(3)	0.0236(5)	0.0276(6)	0.0194(5)	-0.0072(4)	-0.0031(4)	0.0011(4)
Pb11		0.48670(11)	0.23079(6)	0.99463(5)	0.0235(3)	0.0234(5)	0.0232(6)	0.0219(5)	0.0002(4)	-0.0021(4)	0.0035(4)
Sb1A	0.69(7)	0.029(2)	0.1701(3)	0.5736(3)	0.0158(6)						
Sb1B	0.31(7)	-0.004(4)	0.1743(7)	0.5769(6)	0.0158(6)						
Sb2		0.0503(2)	0.9794(1)	0.08083(8)	0.0212(4)	0.0228(9)	0.025(11)	0.0187(9)	-0.0081(7)	-0.0071(7)	0.0094(7)
Sb3	0.741(8)	0.1067(6)	0.0473(3)	0.4045(3)	0.0221(7)						
Pb12	0.259(8)	0.0927(9)	0.0379(5)	0.4095(3)	0.0221(7)						
Sb4A	0.63(3)	0.161(1)	0.3547(2)	0.1324(2)	0.0173(6)						
Sb4B	0.37(3)	0.207(1)	0.3550(3)	0.1312(3)	0.0173(6)						
Sb5		0.2081(2)	0.90797(9)	0.25218(8)	0.0201(4)	0.0242(9)	0.02(1)	0.0145(8)	-0.0029(7)	-0.0004(7)	0.0036(7)
Sb6		0.2112(2)	0.56013(9)	0.09091(8)	0.0203(4)	0.0266(9)	0.018(11)	0.0180(9)	-0.00391(7)	-0.00672(8)	0.0025(7)
Sb7		0.27745(2)	0.43403(9)	0.93941(8)	0.0209(4)	0.0281(9)	0.017(10)	0.0171(8)	-0.0017(7)	-0.0031(7)	0.0004(7)
Sb8		0.2994(2)	0.09129(9)	0.75116(8)	0.0233(4)	0.0251(9)	0.021(11)	0.0202(9)	0.0006(7)	0.0019(7)	0.0028(7)
Sb9		0.3259(2)	0.64833(9)	0.84667(8)	0.0200(4)	0.0251(9)	0.0153(9)	0.0180(8)	-0.0001(7)	-0.0015(7)	-0.0001(7)
Sb10	0.910(8)	0.3889(2)	0.95737(9)	0.59170(7)	0.0215(6)	0.0253(9)	0.0233(11)	0.0162(9)	-0.0080(7)	-0.0022(7)	0.0054(7)
Pb13	0.090(8)	0.3889(2)	0.95737(9)	0.59170(7)	0.0215(6)	0.0253(9)	0.0233(11)	0.0162(9)	-0.0080(7)	-0.0022(7)	0.0054(7)
Sb11		0.3986(2)	0.53266(9)	0.69370(8)	0.0201(4)	0.0225(9)	0.020(10)	0.0189(9)	-0.0062(7)	-0.0036(7)	0.0021(7)
Sb12		0.4466(2)	0.01837(9)	0.92107(8)	0.0234(4)	0.0256(9)	0.028(11)	0.0201(9)	-0.0100(8)	-0.0092(7)	0.0109(8)
Sb13A	0.56(6)	0.508(2)	0.8249(5)	0.4206(3)	0.0173(6)						
Sb13B	0.44(6)	0.475(3)	0.8316(6)	0.4249(4)	0.0173(6)						
S1		0	0.5	0.5	0.020(2)	0.018(4)	0.015(5)	0.027(5)	0.006(4)	-0.007(4)	0.003(4)
S2		0.0135(7)	0.3901(4)	0.0306(3)	0.018(1)	0.019(3)	0.018(4)	0.015(3)	-0.001(3)	-0.003(3)	0.004(3)
S3		0.0163(7)	0.2929(3)	0.4964(3)	0.016(1)	0.021(3)	0.012(4)	0.016(3)	-0.006(3)	-0.001(3)	0.001(3)
S4		0.0504(7)	0.1407(4)	0.8286(3)	0.023(1)	0.027(4)	0.015(4)	0.022(3)	0.001(3)	0.002(3)	0.001(3)
S5		0.0587(7)	0.4716(4)	0.8246(3)	0.023(1)	0.021(3)	0.021(4)	0.026(4)	-0.004(3)	-0.002(3)	-0.001(3)
S6		0.0883(7)	0.6107(4)	0.3226(3)	0.018(1)	0.024(3)	0.022(4)	0.009(3)	-0.003(3)	-0.002(3)	0.001(3)
S7		0.1076(7)	0.1694(4)	0.3232(3)	0.017(1)	0.017(3)	0.023(4)	0.014(3)	-0.005(3)	-0.006(3)	-0.004(3)
S8		0.1224(7)	0.6836(3)	0.7710(3)	0.019(1)	0.026(3)	0.009(4)	0.021(3)	-0.002(3)	-0.001(3)	0.001(3)
S9		0.1447(7)	0.0081(4)	0.6763(3)	0.020(1)	0.024(3)	0.020(4)	0.015(3)	-0.003(3)	-0.004(3)	0.002(3)
S10		0.1941(7)	0.0273(3)	0.1695(3)	0.016(1)	0.020(3)	0.017(4)	0.012(3)	-0.004(3)	-0.005(3)	0.001(3)
S11		0.1990(7)	0.2194(3)	0.1119(3)	0.017(1)	0.021(3)	0.016(4)	0.014(3)	-0.004(3)	-0.003(3)	0.002(3)
S12		0.1982(7)	0.2300(3)	0.6428(3)	0.021(1)	0.037(4)	0.013(4)	0.017(3)	0.001(3)	-0.011(3)	0.003(3)
S13		0.2002(7)	0.6990(3)	0.1040(3)	0.017(1)	0.022(3)	0.014(4)	0.016(3)	0.005(3)	-0.006(3)	0.001(3)
S14		0.2186(7)	0.5589(4)	0.6111(3)	0.022(1)	0.029(4)	0.017(4)	0.020(3)	0.002(3)	-0.010(3)	0.001(3)
S15		0.2269(7)	0.8884(4)	0.5179(3)	0.020(1)	0.020(3)	0.022(4)	0.019(3)	-0.001(3)	-0.005(3)	0.002(3)
S16		0.2447(7)	0.1005(4)	0.9844(3)	0.022(1)	0.027(4)	0.017(4)	0.021(3)	-0.010(3)	0.003(3)	0.006(3)
S17		0.2547(7)	0.8976(4)	0.0174(3)	0.020(1)	0.023(3)	0.016(4)	0.020(3)	-0.003(3)	0.002(3)	0.003(3)
S18		0.2658(7)	0.1143(4)	0.4834(3)	0.023(1)	0.028(4)	0.020(4)	0.020(3)	-0.003(3)	-0.004(3)	0.002(3)
S19		0.3011(7)	0.3077(4)	0.8924(3)	0.018(1)	0.016(3)	0.024(4)	0.014(3)	-0.003(3)	-0.004(3)	0.002(3)
S20		0.3004(7)	0.7731(3)	0.8937(3)	0.017(1)	0.018(3)	0.016(4)	0.017(3)	-0.006(3)	-0.003(3)	0.001(3)
S21		0.3041(7)	0.9703(3)	0.8318(3)	0.016(1)	0.020(3)	0.016(4)	0.013(3)	-0.004(3)	-0.006(3)	-0.002(3)
S22		0.3198(7)	0.7707(4)	0.3543(3)	0.023(1)	0.036(4)	0.019(4)	0.017(3)	-0.003(3)	-0.014(3)	0.002(3)
S23		0.3413(7)	0.4421(4)	0.3905(3)	0.025(2)	0.027(4)	0.014(4)	0.030(3)	0.003(3)	0.004(3)	-0.001(3)
S24		0.3587(7)	0.9912(4)	0.3220(3)	0.024(2)	0.025(4)	0.024(4)	0.023(3)	0.001(3)	-0.007(3)	0.001(3)
S25		0.3941(7)	0.5282(4)	0.1750(3)	0.021(1)	0.023(3)	0.014(4)	0.026(3)	-0.006(3)	-0.005(3)	0.005(3)
S26		0.3950(7)	0.8351(4)	0.6721(3)	0.017(1)	0.021(3)	0.017(4)	0.015(3)	-0.002(3)	-0.006(3)	0.004(3)
S27		0.4055(7)	0.3158(4)	0.2318(3)	0.022(1)	0.024(3)	0.015(4)	0.023(3)	-0.004(3)	0.003(3)	0.003(3)
S28		0.4057(7)	0.3920(4)	0.6850(3)	0.017(1)	0.020(3)	0.019(4)	0.015(3)	-0.007(3)	-0.004(3)	-0.001(3)
S29		0.4561(7)	0.3902(3)	0.0275(3)	0.019(1)	0.023(3)	0.0134)	0.018(3)	-0.001(3)	-0.003(3)	0.002(3)
S30		0.4594(7)	0.8598(4)	0.1711(3)	0.021(1)	0.027(3)	0.020(4)	0.015(3)	-0.003(3)	-0.002(2)	0.001(3)
S31		0.4830(7)	0.7112(4)	0.5056(3)	0.017(1)	0.020(3)	0.022(4)	0.010(3)	-0.002(3)	-0.004(3)	0.004(3)

The S1 site is the site of chlorine.

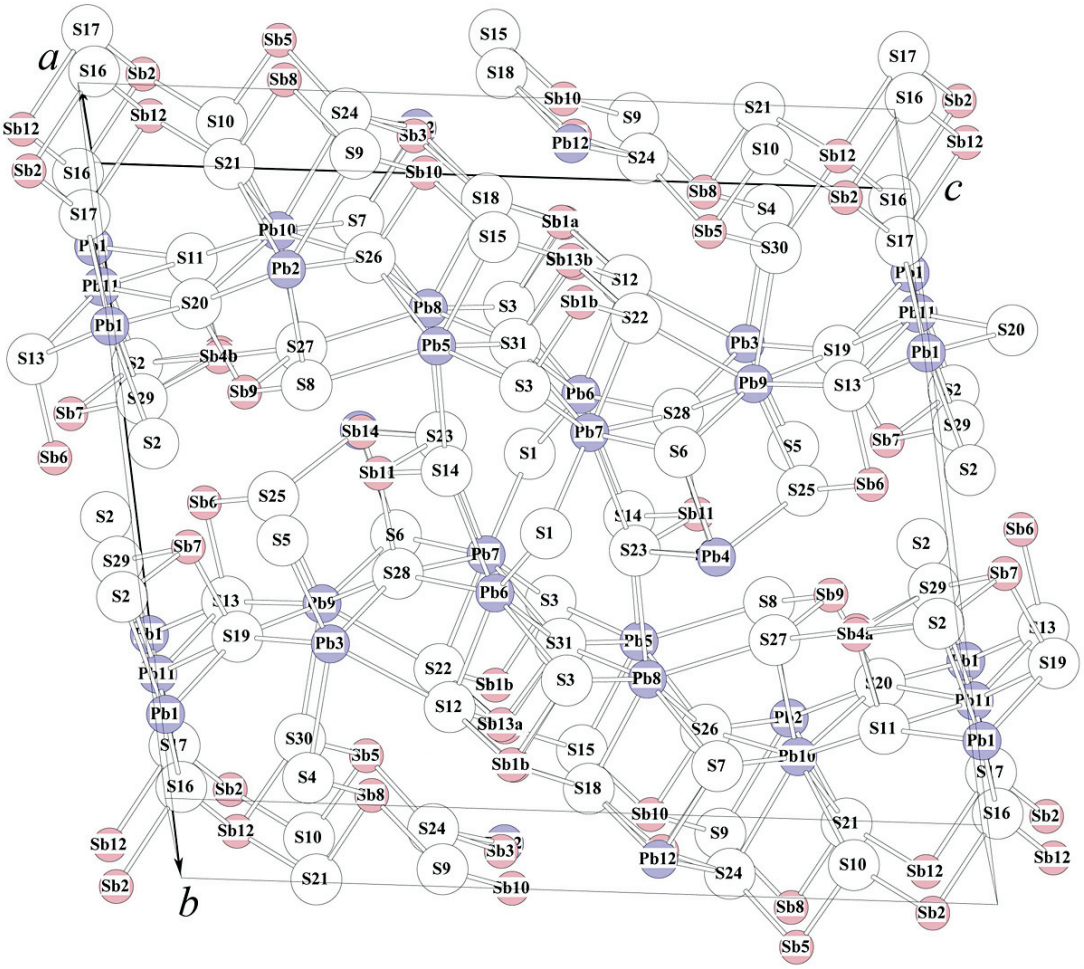

FIG. 2. The contents of the $a \approx 8$ Å unit cell of dadsonite. For the details of the Sb–S mesh, see also Figures 3a and 3b. The S1 site is the site of chlorine.

the values of their volume-based eccentricity, because the monocapped trigonal prisms of Pb can be better fitted by a sphere circumscribed to their S ligands than the bicapped trigonal prisms of Pb1, 2, 6, 7, 10, and 11 (Table 5). The bicapped trigonal–prismatic coordinations of lead (Figs. 1, 2) have a slightly more symmetrical distribution of cation–anion distances (Table 4), one capping distance being among the shortest, another one among the long distances, *e.g.*, 2.90 Å and 3.20 Å for Pb2.

If one plots the opposing lead–sulfur distances from the Pb coordination-polyhedra onto the bond-length hyperbola of Berlepsch *et al.* (2001a), originally defined for Pb in the meneghinite homologues, their values are scattered symmetrically around the central portions of this hyperbola (Fig. 4). Only the bridging Pb–S distance of substituting Pb4 and Pb12 deviates from this trend, as an adjustment to the lone-electron-pair micelle of Sb in the Type-5 and Type-3 layers, respectively. In addition, the Pb–S distances for the mixed sites, and especially for the minor Pb12 position, reflect the fact that all of the S positions involved are a weighted average of the S positions belonging to the Sb-occupied and Pb-occupied versions of the same mixed-cation polyhedron. The weights are the respective cation-occupancies, *i.e.*, 0.65Pb and 0.35Sb for Pb4, and 0.74Sb and 0.26Pb in the case of Pb12. Therefore, the bond-length values for these mixed cations, in Table 4, can be considered of orientational value only. The volume-based eccentricity of these sites approaches that of the Sb coordination

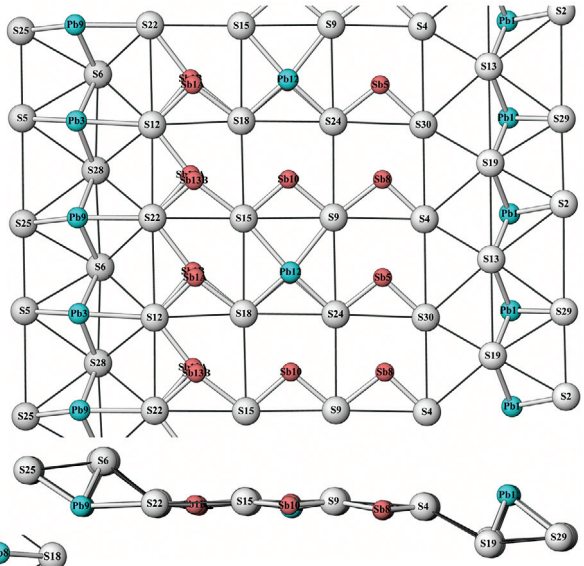

FIG. 3a. The Sb–S mesh representing the bases of square coordination pyramids [SbS_5] in the Type-3 layer, and the adjacent Pb sites. Pb12 nearly overlaps the principal Sb3 site. The situation of the slice can be seen in Figure 3c.

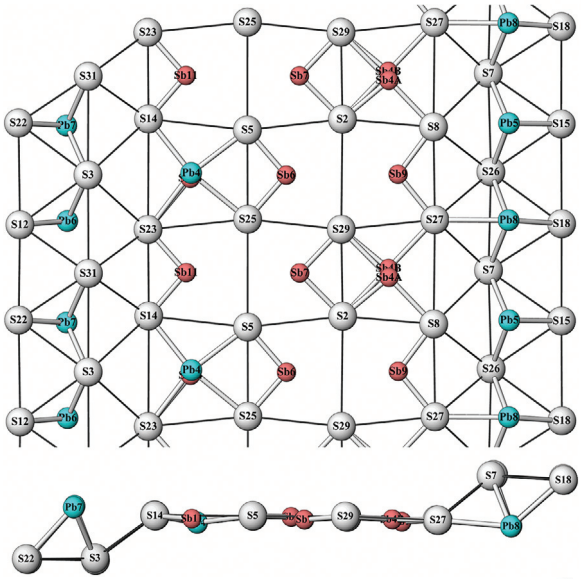

FIG. 3b. The Sb–S mesh representing the bases of trapezoidally distorted "square" coordination pyramids [SbS_5] in the Type-5 layer, and the adjacent Pb sites. Atom Pb4 overlaps the minor Sb14 site. The position of this slice in the structure of dadsonite can be seen in Figure 3c.

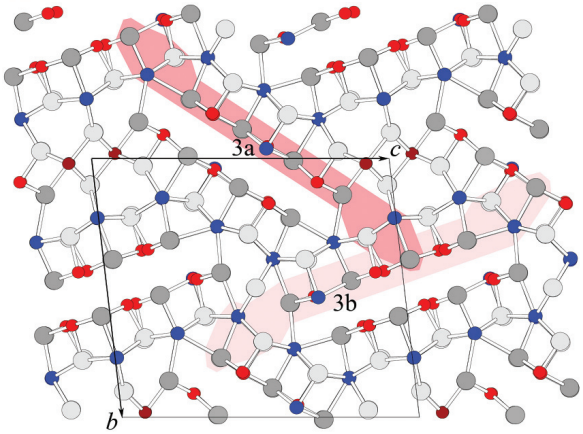

FIG. 3c. Situation of the sections illustrated in Figures 3a and 3b.

(Table 5). The Pb13 site, with only 0.09Pb, overlapping with the Sb10 site, which shows 0.91Sb, was refined using the same positional parameters as obtained for the majority cation Sb10.

The coordination polyhedra of antimony fall in three groups. For the first of them, comprising Sb5, 6, 7, 9, and 11, three short bonds (2.42–2.59 Å) are combined with three to four long Sb–S distances, starting at 3.09 Å or, for Sb11, even at 3.44 Å (Table 4). With the exception of Sb5, all these Sb atoms form [SbS_5] coordination pyramids with trapezoidal bases (a square base is present for Sb5) in the Type-5 layer (Fig. 3). The two largest Sb–S distances span the lone-electron-pair micelle that separates the two triple ribbons of Sb polyhedra, situated back-to-back in each rod.

The other set of empirical Sb–S bond distances (Sb1A and B, 2, 4A, 4B, 8, 12, 13A, and 13B) shows three regularly increasing short distances, starting at 2.41–2.45 Å and increasing to 2.60–2.72 Å. The Sb1A–1B, 4A–4B, and 13A–13B sites are split Sb-sites, which in the unsplit form exhibit augmented U_{iso} values, distinctly elongate displacement-ellipsoids, and also manifest an average bond-length atypical for Sb. Splitting of these positions using an isotropic displacement parameter separates at least partly the two subsites, revealing their unequal occupancies. Such split sites will have a nearly equal bond-length to the vertex of the [SbS_5] coordination pyramid (*e.g.*, for Sb13A and B, it is 2.42 Å and 2.41 Å, respectively). They will also have one more-or-less common, short Sb–S distance to one S atom in the square base of the pyramid (for Sb13A and B, it is the distance to S22, at 2.48 and 2.41 Å), and will have one long Sb–S distance that opposes this bond (to S18 at 3.18 and 3.28 Å, respectively). The other short Sb–S bond of the split Sb half-atom invariably overlaps the long Sb–S distance of its split counterpart (2.70 and 2.69 Å, respectively, for Sb13A and B, overlapping with the distances 2.96–2.99 Å).

As illustrated for Sb13, it is not possible to determine the correct Sb–S distances for all three polyhedra in which there is splitting of cation positions, presumably because of the imperfect separation of two closely overlapping Sb positions in the refinement, and because of the averaging of the positions of the sulfur ligands

TABLE 4. CATION – LIGAND DISTANCES (Å) IN DADSONITE

Pb1-		Pb2-		Pb3-		Pb4-		Sb14-		Pb5-		Pb6-		Pb7-		Pb8-		Pb9-	
S20	2.870(5)	S7	2.873(7)	S5	2.792(7)	S6	2.686(8)	S6	2.692(11)	S31	2.865(5)	S6	2.884(5)	S6	2.837(7)	S31	2.837(7)	S25	2.799(7)
S13	2.892(6)	S8	2.901(5)	S6	2.935(6)	S14	2.913(6)	S23	2.812(12)	S3	2.928(7)	S1	2.972(1)	S22	2.944(7)	S18	2.953(6)	S28	2.886(6)
S2	2.962(7)	S26	2.936(5)	S28	2.969(5)	S5	2.999(7)	S25	2.988(10)	S15	2.938(6)	S12	2.983(7)	S1	3.024(1)	S3	2.955(5)	S19	2.944(5)
S16	3.068(7)	S11	3.012(5)	S19	2.980(6)	S23	3.008(7)	S14	3.069(10)	S26	3.027(6)	S3	3.026(6)	S28	3.084(5)	S26	3.038(5)	S13	3.021(6)
S17	3.083(7)	S21	3.166(6)	S13	2.989(5)	S25	3.093(6)	S5	3.165(12)	S7	3.070(6)	S28	3.026(7)	S3	3.089(5)	S7	3.084(7)	S6	3.044(5)
S19	3.134(5)	S9	3.204(6)	S4	3.227(7)	S8	3.658(7)	S27	3.558(11)	S14	3.109(7)	S14	3.122(7)	S31	3.139(7)	S23	3.087(7)	S22	3.215(7)
S11	3.135(7)	S10	3.251(5)	S12	3.257(6)	S27	3.681(7)	S8	3.800(12)	S8	3.207(6)	S31	3.263(6)	S23	3.163(7)	S27	3.131(6)	S30	3.249(7)
S4	3.692(7)	S20	3.271(6)											S14	3.506(6)				

Pb10-		Pb11-		Sb2-		Sb3-		Pb12-		Sb9-		Sb5-		Sb6-		Sb7-		Sb8-	
S27	2.866(7)	S29	2.911(6)	S17	2.423(6)	S7	2.503(8)	S24	2.665(9)	S20	2.439(6)	S10	2.498(5)	S13	2.454(6)	S19	2.464(7)	S21	2.486(5)
S7	2.893(5)	S11	2.927(5)	S10	2.514(7)	S18	2.599(9)	S7	2.672(10)	S27	2.463(5)	S30	2.529(6)	S25	2.469(7)	S29	2.541(6)	S4	2.491(6)
S26	2.925(7)	S19	2.958(6)	S4	2.603(6)	S24	2.604(8)	S18	2.692(11)	S8	2.491(7)	S24	2.590(7)	S5	2.509(5)	S2	2.574(5)	S9	2.679(7)
S20	3.090(5)	S13	3.062(5)	S16	2.914(6)	S9	3.085(9)	S9	3.004(11)	S2	3.307(5)	S4	3.089(7)	S29	3.257(5)	S25	3.157(5)	S30	2.935(7)
S11	3.135(6)	S17	3.066(6)	S21	3.231(6)	S15	3.116(7)	S15	3.065(10)	S29	3.344(7)	S22	3.187(7)	S2	3.342(7)	S5	3.172(7)	S12	3.244(7)
S10	3.210(6)	S20	3.071(7)	S16	3.363(7)	S15	3.605(8)	S15	3.484(10)	S25	3.829(7)	S9	3.352(6)	S29	3.739(6)	S2	3.887(7)	S24	3.280(6)
S24	3.230(6)	S16	3.095(7)	S17	3.947(7)					S5	3.925(7)			S2	3.812(7)	S29	3.981(6)		
S21	3.249(5)	S30	3.695(7)																

Sb10-, Pb13-		Sb11-		Sb12-		Sb1A-		Sb1B-		Sb4A-		Sb4B-		Sb13A-		Sb13B-	
S26	2.502(5)	S14	2.417(7)	S16	2.413(6)	S12	2.452(13)	S3	2.434(13)	S11	2.436(6)	S11	2.434(8)	S31	2.415(10)	S22	2.405(15)
S9	2.543(6)	S23	2.430(5)	S21	2.518(7)	S3	2.486(8)	S12	2.573(28)	S2	2.557(9)	S29	2.592(12)	S22	2.481(15)	S31	2.483(11)
S15	2.561(7)	S28	2.472(6)	S30	2.632(6)	S18	2.600(11)	S18	2.838(24)	S8	2.720(9)	S2	2.795(14)	S12	2.701(15)	S15	2.695(13)
S24	3.140(7)	S25	3.438(7)	S17	2.901(6)	S22	3.150(14)	S22	2.881(28)	S29	2.862(9)	S27	2.835(14)	S15	2.963(13)	S12	2.991(15)
S18	3.228(6)	S5	3.466(5)	S10	3.261(6)	S15	3.281(14)	S15	3.154(27)	S27	3.102(10)	S8	3.017(14)	S18	3.178(15)	S18	3.276(16)
S18	3.532(7)	S27	3.696(7)	S17	3.380(7)	S9	3.510(10)	S9	3.643(19)	S5	3.594(9)	S25	3.669(12)	S24	3.638(12)	S24	3.484(13)
		S8	3.697(6)	S16	3.895(7)					S25	3.861(9)	S5	3.779(12)				

belonging to the two alternative Sb configurations. The bond distances influenced by these errors deviate from the bond-length hyperbola established for Sb by Berlepsch *et al*. (2001a) and lie along a straight line originating at the point defined as the 2.50 Å/3.27 Å ratio of opposing bond-lengths (Fig. 4), with the equation: $y = 7.86\ (0.32) - 1.83\ (0.13)\ x$, where x and y, respectively, are the shorter and the opposing longer cation–ligand distances, and values within parentheses are the standard deviations of the coefficients of the equation.

This "hyperbola secant" trend is typical for split positions, as already established for Pb–As sulfosalts by Berlepsch *et al*. (2001b). It suggests that Sb8 also is a split position, although it was left as a single atom because the largest U_{ii} value observed is less than 0.03, an empirical cut-off limit used for cation splitting in the last stages of the current refinement of the structure.

For the sites Sb2 and Sb12, a different explanation of the gradation of short Sb–S distances is required. As a result of its position at the ends of atomic arrays in the rods of the Type-3 layer, the column Sb2–Sb12 of Sb coordination-pyramids forms an unusually tight double column, conjugated with respect to the column Sb5–Sb8. As a result of overbonding and, possibly, also of the Sb–Sb repulsion, all of the short distances appear somewhat augmented and altered in comparison to the distances in the first category of Sb polyhedra treated here. In particular, the Sb–S bond to the vertex of the square pyramid is the third shortest bond in the polyhedra of Sb2 and Sb12.

TABLE 5. DISTORTION PARAMETERS FOR THE CATION POLYHEDRA IN DADSONITE

Atom	1	2	3	4	5	6	7	8	9
Pb1	3.091	0.101	0.940	0.048	0.273	0.820	123.72	51.08	2.09
Pb2	3.079	0.079	0.974	0.035	0.220	0.922	122.22	51.11	2.10
Pb3	3.027	0.085	0.992	0.091	0.234	0.976	116.20	39.98	2.12
Sb14	3.165	0.199	0.978	0.150	0.486	0.934	132.78	42.72	1.54
Pb4	3.165	0.190	0.978	0.150	0.469	0.934	132.78	42.72	1.98
Pb5	3.027	0.060	0.990	0.115	0.168	0.969	116.17	38.89	2.05
Pb6	3.076	0.073	0.986	0.151	0.203	0.958	121.89	39.16	1.95
Pb7	3.113	0.100	0.972	0.078	0.270	0.916	126.33	50.47	2.02
Pb8	3.016	0.050	0.988	0.111	0.143	0.964	114.97	38.66	2.08
Pb9	3.029	0.088	0.994	0.093	0.240	0.982	116.36	39.96	2.12
Pb10	3.076	0.082	0.986	0.035	0.226	0.958	121.95	51.02	2.10
Pb11	3.085	0.099	0.943	0.046	0.268	0.829	122.95	50.86	2.09
Sb1A	3.019	0.273	0.970	0.159	0.616	0.911	115.22	30.83	2.88
Sb1B	3.019	0.253	0.970	0.159	0.583	0.911	115.22	30.83	2.61
Sb2	2.980	0.277	0.964	0.146	0.621	0.891	110.82	35.84	3.09
Pb12	3.015	0.185	0.962	0.149	0.459	0.886	114.77	31.09	2.76
Sb3	3.015	0.252	0.962	0.149	0.581	0.886	114.77	31.09	2.58
Sb4A	3.010	0.273	0.964	0.132	0.616	0.893	114.28	37.56	2.84
Sb4B	3.010	0.266	0.964	0.132	0.605	0.893	114.28	37.56	2.75
Sb5	2.970	0.235	0.982	0.166	0.552	0.946	109.72	29.13	2.77
Sb6	3.071	0.314	0.975	0.128	0.677	0.926	121.35	40.04	3.05
Sb7	3.159	0.324	0.959	0.179	0.691	0.877	131.99	41.00	2.79
Sb8	2.935	0.223	0.983	0.144	0.532	0.949	105.90	28.86	2.83
Sb9	3.147	0.346	0.968	0.179	0.720	0.904	130.51	40.54	3.12
Sb10, Pb13	3.039	0.266	0.970	0.177	0.604	0.909	117.56	30.80	3.56
Sb10	3.039	0.266	0.970	0.177	0.604	0.909	117.56	30.80	2.72
Sb11	3.071	0.320	0.991	0.124	0.686	0.974	121.28	40.23	3.29
Sb12	2.981	0.270	0.969	0.145	0.611	0.907	110.94	35.88	3.06
Sb13A	2.993	0.268	0.970	0.163	0.608	0.910	112.29	29.93	2.96
Sb13B	2.993	0.265	0.970	0.163	0.602	0.910	112.29	29.93	2.96

Column headings: 1: sphere radius (Å), 2: eccentricity, 3: sphericity, 4: volume distortion (%), 5: volume eccentricity, 6: volume sphericity (Å^3), 7: sphere volume (Å^3), 8: polyhedron volume (Å^3), 9: bond valence. Distortion parameters are defined in Balić-Žunić & Makovicky (1996) and Makovicky & Balić-Žunić (1998).

The Sb sites substituted by lead are best recognized in the bond-hyperbola plot. Instead of the linear trend observed for the split sites, the data points belonging to these sites lie on hyperbolas intermediate between those of Sb and Pb (Fig. 4). The points for Sb10 and Sb3 lie closest to the Sb hyperbola, in agreement with a low degree of Pb substitution in these sites; the minority Pb12 follows this trend. Minor Sb14 is closest to the Pb hyperbola, whereas its complement, Pb4, is in the cluster of Pb values, except for the out-of-plane Pb–S distances across the lone-electron-pair micelle. Thus, in accordance with the weighted average character of the sulfur ligands, the Pb:Sb ratio in the polyhedra has a greater influence on the position of the cation hyperbola than does the nature of the cation itself.

The deviations of the data points belonging to the split or mixed cation sites from the simple hyperbolic trend are paralleled by unrealistic bond-valence values (Table 5) for these sites, at variance with the acceptable values obtained for all Pb and Sb polyhedra that do not exhibit such complex configurations. Bond-valence calculations confirm that the S1 site is the site of chlorine, with a bond valence total of 1.1 valence units (*vu*).

Order–Disorder Character of Dadsonite

If we preserve the orientation of axes defined for the unit cell, the Type-3_{SnS} layer has the ideal layer-symmetry $p\bar{1}$ with the a' axis one half of the a value of the unit cell. The type-5 layer has the ideal layer-symmetry $b2/m11$, with the c parameter equal to $2\mathbf{c} - \mathbf{a}$ of the triclinic unit-cell.

The γ angle of the unit-cell, 89.2°, indicates a slight obliquity of the structure, which arises where the consecutive (010) rod-layers are stacked along the [010] direction. After every Type-5 layer with its horizontal mirror planes, there is a choice between a continuation of this triclinic stagger in the $+\vec{a}$ or in the $-\vec{a}$ direction. A change in the sense of stagger means a twinning on the (010) system of planes as a twin element, and in the extreme case of the $+a\ -a\ +a\ -a$ stagger, a monoclinic structure with a b glide plane (100) and a doubled b axis results.

The halved repetition-period $a/2$ of Type-3 layer means that the consecutive Type-5 layer can attach itself either at (practically) the same x height as the Type-5 layer immediately preceding the Type-3 layer in question, or it can attach itself at $(x + 0.5)$ instead. A consistent application of the $(x + 0.5)$ stacking principle would lead to a triclinic C-centered cell with a

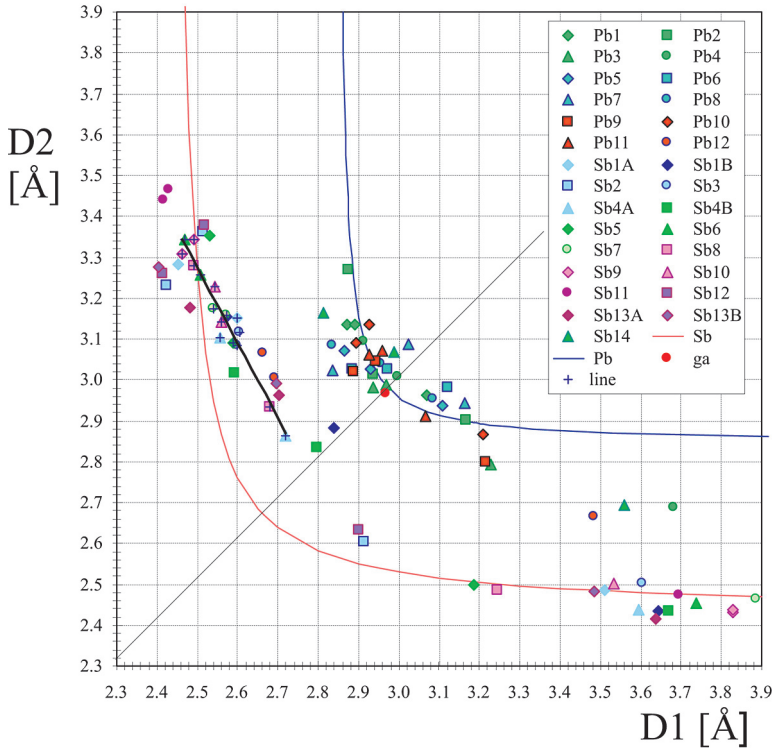

FIG. 4. Element-specific bond-length hyperbolae for the pairs of opposing bonds and distances in the Sb and Pb coordination polyhedra of dadsonite. The upper-left-hand part of the diagram contains pairs of bonds from the bases of square coordination-pyramids; the lower-right-hand side comprises bonds to the vertex of the coordination pyramids, opposed by the shortest cation–anion distance below the base of the pyramid. Bond-length hyperbolae are from Berlepsch *et al.* (2001a) (Sb) and Topa (2001) (Pb); the linear trend is discussed in the text. The PbS value for galena is denoted as "ga". Points used to calculate the linear trend given in the text are indicated by crosses.

doubled *b* axis, preserving the remaining parameters of the original cell.

In both types of disorder, the difference in internal energy will be minimal, because the layers subject to disorder act upon one another *via* an intermediate layer with heightened symmetry or periodicity. These errors were perhaps the chief factors that impeded further refinement of the Saint-Pons material by Mumme and Makovicky (in Makovicky 1993). They appear little-active in the current material, the principal reason being that both the double periodicity of the Type-3 layer and the *b*2/*m* symmetry of the Type-5 layer are only approximate, violated to a small but constant extent. Therefore, we deal with a *desymmetrized* OD structure in which the OD phenomena are present only as occasional, twinning or antiphase-boundary events (Ďurovič 1979).This twinning is typical of dadsonite in polished sections under crossed polars and helps to distinguish it from other Pb–Sb sulfosalts (Moëlo 1983). We can speculate that the frequency of the events might be influenced by variations in the chemical composition of dadsonite, namely the variation in the concentration of Pb in some of the columns of Sb coordination-pyramids, destroying the periodicities described above and layer symmetries.

COMPARISON OF THE 8 Å STRUCTURE AND 4 Å SUBSTRUCTURE

Many lead–antimony sulfosalts exhibit a pronounced ~4 Å substructure, producing a subset of strong X-ray reflections, and an 8 Å superstructure that modifies the 4 Å submotif by substitutions, occupation of alternative positions in a coordination polyhedron or, perhaps in

some cases, vacancies, producing weak to very weak reflections.

The intensity of the generally weak 8 Å reflections varies with the extent of modifications present in the structure (mineral species), with the potential disorder of these phenomena along the 4 Å direction, as well as with the perfection and size of the crystal investigated. Some sulfosalts, *e.g.*, jamesonite, $FePb_4Sb_6S_{14}$ (Léone *et al*. 2003), or robinsonite, $Pb_4Sb_6S_{13}$ (Makovicky *et al*. 2004), have only a 4 Å periodicity. These latest refinements confirm the results of the previous ones (*e.g.*, Niizeki & Buerger 1957, Skowron & Brown 1990a, Franzini *et al*. 1992) with respect to the absence of the superstructure. Others, like boulangerite, $Pb_5Sb_4S_{11}$, may have both the ordered variants (Mumme 1989) and disordered (synthetic) variants (*e.g.*, Petrova *et al*. 1978, Skowron & Brown 1990b) of the Pb–Sb substitution schemes. Finally, for zinkenite, $\sim Pb_9Sb_{22}S_{42}$, both ordered and disordered 8 Å variants are known, but the hitherto published determinations of its structure (*e.g.*, Portheine & Nowacki 1975) treated only the 4 Å substructure. Studies of the 8 Å variants are currently being performed by us, however. The remarkable oxy-sulfosalts from Bucca della Vena, in Italy (*e.g.*, scainiite, $Pb_{14}Sb_{30}S_{54}O_5$, Moëlo *et al*. 2000) show very weak 8-Å levels.

In light of the above situation, how much information may be lost by analyzing only the 4-Å substructure? The current study allows us to compare the 8-Å refinement with the results of the substructure refinement (Table 2, 6 and 7, Fig. 5), which achieved an R_1 of 4.94% using the subset of 3531 reflections [with F_o

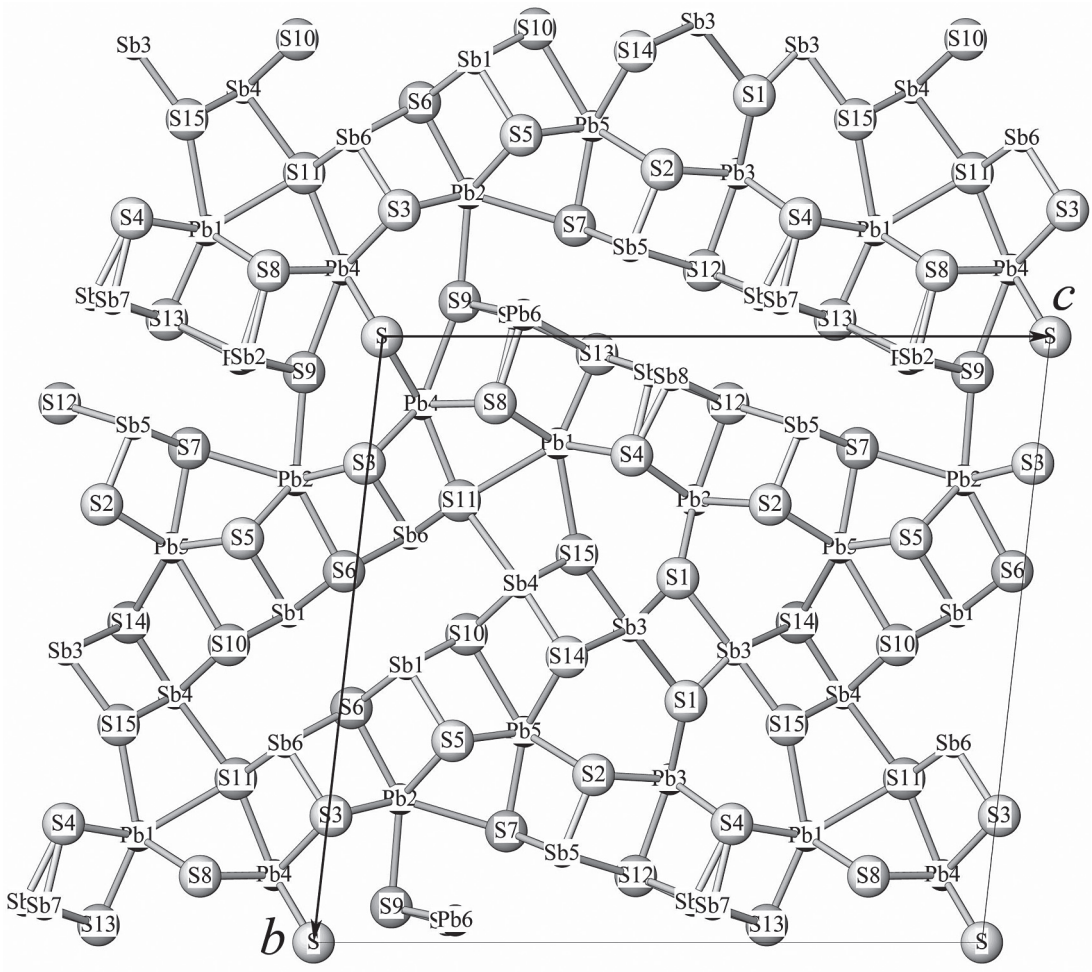

FIG. 5. The 4-Å substructure of dadsonite projected along [100]; it is to be compared with the projection of the 8-Å structure in Figure 1. The S1 site is the site of chlorine.

TABLE 6. POSITIONAL AND DISPLACEMENT PARAMETERS FOR THE 4 Å STRUCTURE OF DADSONITE

ATOM	*sof*	*x*	*y*	*z*	*U*eq	U_{11}	U_{22}	U_{33}	U_{23}	U_{13}	U_{12}
Pb1		0.48704(18)	0.17595(5)	0.28094(4)	0.0213(2)	0.0234(5)	0.0212(5)	0.0193(4)	0.0029(4)	0.0000(4)	-0.0006(3)
Pb2		0.46610(18)	0.76339(5)	0.10512(4)	0.0229(2)	0.0229(5)	0.0280(5)	0.0181(4)	0.0040(4)	0.0006(4)	-0.0004(4)
Pb3		0.47037(19)	0.26952(5)	0.49481(4)	0.0238(2)	0.0250(5)	0.0234(5)	0.0221(5)	-0.0010(4)	0.0018(4)	-0.0036(3)
Pb4		0.50672(19)	0.11125(5)	0.07055(4)	0.0287(3)	0.0279(5)	0.0344(6)	0.0240(5)	0.0040(4)	-0.0006(4)	0.0030(4)
Pb5		0.45958(18)	0.65206(5)	0.27908(4)	0.0246(2)	0.0243(5)	0.0308(6)	0.0198(4)	0.0075(4)	0.0018(4)	0.0027(4)
Sb1		0.88034(30)	0.54324(8)	0.09268(7)	0.0155(3)	0.0194(7)	0.0169(8)	0.0115(6)	0.0077(6)	0.0006(6)	-0.0024(5)
Sb2	0.715(8)	0.98781(91)	0.9657(2)	0.1967(2)	0.0197(6)						
Pb6	0.285(8)	0.99357(13)	0.9634(3)	0.2084(3)	0.0197(6)						
Sb3		0.31642(32)	0.48052(9)	0.42005(7)	0.0229(4)	0.0230(7)	0.0264(9)	0.0204(8)	0.0092(7)	-0.0040(6)	-0.0086(6)
Sb4		0.84048(33)	0.40830(8)	0.24935(7)	0.0231(4)	0.0293(8)	0.0203(9)	0.0192(7)	0.0010(6)	0.0062(6)	-0.0029(6)
Sb5		0.00636(39)	0.85307(9)	0.35688(9)	0.0414(5)	0.0396(9)	0.0163(9)	0.069(1)	0.0093(9)	0.0089(9)	0.0014(7)
Sb6		0.10149(35)	0.32827(9)	0.07603(7)	0.0250(4)	0.0362(8)	0.0200(9)	0.0186(8)	0.0001(6)	-0.0057(7)	0.0068(6)
Sb7	0.49(1)	0.98638(72)	0.0601(2)	0.4089(4)	0.022(1)						
Sb8	0.51(1)	0.99359(72)	0.0661(2)	0.4392(4)	0.023(1)						
S		0	0	0	0.096(5)						
S1		0.973(1)	0.3986(3)	0.4835(3)	0.021(1)	0.026(3)	0.017(3)	0.021(3)	0.006(2)	0.005(2)	-0.004(2)
S2		0.992(1)	0.7232(3)	0.3907(3)	0.019(1)	0.021(3)	0.019(3)	0.018(3)	0.008(2)	0.001(2)	0.000(2)
S3		0.972(1)	0.7910(3)	0.0049(3)	0.018(1)	0.020(3)	0.019(3)	0.014(3)	0.005(2)	0.001(2)	0.000(2)
S4		0.995(1)	0.1956(3)	0.3940(3)	0.019(1)	0.018(3)	0.022(3)	0.016(3)	0.001(2)	-0.001(2)	-0.001(2)
S5		0.962(1)	0.6671(3)	0.1743(3)	0.019(1)	0.018(3)	0.021(3)	0.019(3)	0.005(2)	-0.003(2)	0.001(2)
S6		0.477(1)	0.6126(3)	0.0171(3)	0.022(1)	0.023(3)	0.021(3)	0.021(3)	0.001(2)	-0.001(2)	-0.002(2)
S7		0.488(1)	0.8162(3)	0.2697(3)	0.026(1)	0.042(3)	0.014(3)	0.023(3)	0.004(2)	0.008(3)	-0.000(2)
S8		0.999(1)	0.1091(3)	0.1811(3)	0.020(1)	0.020(3)	0.022(3)	0.018(3)	0.004(2)	-0.001(2)	-0.000(2)
S9		0.488(1)	0.9418(3)	0.1107(3)	0.051(1)	0.113(6)	0.014(4)	0.025(3)	-0.002(3)	0.007(4)	-0.000(4)
S10		0.463(1)	0.4913(3)	0.1770(3)	0.023(1)	0.027(3)	0.023(3)	0.018(3)	0.001(2)	-0.001(2)	-0.001(2)
S11		0.522(1)	0.2705(3)	0.1441(3)	0.023(1)	0.037(3)	0.014(3)	0.018(3)	0.002(2)	-0.010(2)	-0.003(2)
S12		0.499(1)	0.8901(3)	0.4707(3)	0.044(1)	0.097(3)	0.016(3)	0.018(3)	0.001(2)	0.007(3)	-0.003(2)
S13		0.489(1)	0.0288(3)	0.3249(3)	0.037(1)	0.070(4)	0.016(3)	0.025(3)	0.005(3)	0.001(3)	-0.002(3)
S14		0.941(1)	0.5285(3)	0.3311(3)	0.016(1)	0.020(3)	0.015(3)	0.014(3)	0.004(2)	-0.002(2)	0.001(2)
S15		0.419(1)	0.3592(3)	0.3285(3)	0.023(1)	0.031(3)	0.017(3)	0.020(3)	-0.001(2)	0.003(2)	-0.003(2)

sof: site-occupancy factor. The S site is the site of chlorine.

TABLE 7. CATION – LIGAND DISTANCES (Å) IN 4 Å DADSONITE

Pb1-		Pb2-		Pb3-		Pb4-		Pb5-		Pb6-		Sb8-	
S13	2.782(6)	S3	2.881(4)	S2	2.898(4)	S8	2.929(5)	S7	2.880(5)	S8	2.646(8)	S4	2.502(16)
S8	2.914(5)	S3	2.909(4)	S12	2.927(6)	S11	2.959(5)	S5	2.903(5)	S9	2.770(9)	S12	2.736(20)
S4	2.963(4)	S6	2.948(5)	S4	2.928(4)	S8	2.978(5)	S5	2.917(5)	S9	2.794(9)	S12	2.741(20)
S4	2.997(4)	S5	3.051(5)	S1	3.067(5)	CL	3.040(1)	S2	3.050(4)	S13	3.128(8)	S13	3.019(23)
S8	3.011(5)	S5	3.054(5)	S1	3.089(5)	CL	3.042(1)	S14	3.188(5)	S13	3.179(8)	S13	3.035(23)
S15	3.230(5)	S9	3.090(5)	S4	3.099(4)	S3	3.082(5)	S2	3.202(4)	S7	3.587(8)	S12	3.763(12)
S11	3.240(6)	S7	3.168(6)	S2	3.104(4)	S9	3.129(6)	S10	3.224(5)	S7	3.596(8)	S12	3.836(12)
				S15	3.697(6)	S3	3.175(5)	S14	3.251(5)				
						S9	3.472(6)						

Sb1-		Sb2-		Sb3-		Sb4-		Sb5-		Sb6-		Sb7-	
S5	2.530(5)	S8	2.547(6)	S1	2.419(6)	S14	2.491(5)	S2	2.418(6)	S3	2.453(5)	S4	2.411(13)
S10	2.584(6)	S9	2.641(8)	S14	2.517(5)	S15	2.510(6)	S7	2.637(6)	S11	2.463(6)	S13	2.621(21)
S6	2.601(6)	S9	2.651(8)	S15	2.624(5)	S10	2.634(6)	S7	2.738(6)	S6	2.759(6)	S13	2.655(20)
S10	3.094(6)	S13	3.285(7)	S1	2.908(5)	S15	3.011(6)	S12	2.994(7)	S11	2.944(5)	S12	3.114(24)
S6	3.158(5)	S13	3.305(7)	S14	3.246(5)	S11	3.216(5)	S12	3.041(7)	S6	3.224(6)	S12	3.162(24)
S6	3.543(5)	S7	3.699(7)	S1	3.372(5)	S10	3.314(5)	S13	3.735(6)	S10	3.554(5)	S12	3.843(16)
		S7	3.734(7)	S1	3.921(5)			S13	3.857(6)			S12	3.949(16)

$> 4\sigma(F_o)$] from the full set used for the 8-Å structure. The same absorption-correction as for the 8 Å structure was used.

In the Type-3 layers, neither statistical splitting nor partial substitution of the Sb position by Pb is visible in the 4-Å substructure. Only details of the bonding scheme (Table 7, Fig. 5) suggest a possible complication in the cation site for the marginal Sb sites Sb4 and Sb6. The lower U_{eq} value of Sb1 indicates a possible admixture of a heavier atom at the Sb1 site. The Sb sites of the Type-5 layer are all split in the 8-Å structure, and one marginal column of cation polyhedra (those of Sb11–Pb4) displays a nearly regular Pb–Sb alternation. The 4-Å substructure of this layer shows more distinct indications of these phenomena than that of the Type-3 layer. The marginal Sb5 has a high U_{eq} value and an unusual scheme of short bonds, a full split of the Sb7–Sb8 position in the central row of polyhedra, as well as a mixture of 0.3Pb and 0.7Sb in the other marginal site. No complications occur in the pure Pb sites of the 4-Å substructure; each of them is an average of two very similar Pb polyhedra from the 8-Å structure.

Summing up these observations, a majority of features observed in the 8-Å structure are already suggested by the 4-Å substructure, but to a lesser degree. Without any knowledge of the 8-Å structure, several of them might be overlooked or not analyzed in detail. Thus, the 4-Å structure is potentially poorer, owing to the omission of coordination or occupancy details of the Sb sites (in our case four out of seven sites). This analysis results in a word of caution: unusual schemes of bonding and bond-valence totals for Sb, as already pointed out by Moëlo *et al*. (2000), are not real coordinations; they are a result of an unresolved overlap of (at least) two split, partly occupied Sb positions inside the same coordination-polyhedron. Full resolution of all details of these overlapping coordinations may not be possible because of the statistical nature of their ligands. Before, and even after, any resolution into their components, these positions will deviate from the Sb trend in the plot of bond-distance hyperbolas and will give false bond-valence values. The same is true for the mixed (Sb, Pb) polyhedra.

Acknowledgements

We gratefully acknowledge the financial support of The Austrian Science Foundation and Danish Research Council for Natural Science. The manuscript benefitted from comments of Drs. J.L. Jambor and Y. Moëlo, as well as from the editorial care of Prof. Robert F. Martin.

References

Balić-Žunić, T. & Makovicky, E. (1996): Determination of the centroid or 'the best centre' of a coordination polyhedron. *Acta Crystallogr*. **B52**, 78-81.

Balić-Žunić, T. & Vicković, I. (1996): IVTON: a program for the calculation of geometrical aspects of crystal structures and some crystal chemical applications. *J. Appl. Crystallogr.* **29**, 305-306.

Berlepsch, P., Makovicky, E. & Balić-Žunić, T. (2001a): Crystal chemistry of meneghinite homologues and related sulfosalts. *Neues Jahrb. Mineral., Monatsh*., 115-135.

Berlepsch, P., Makovicky, E. & Balić-Žunić, T. (2001b): Crystal chemistry of sartorite homologues and related sulfosalts. *Neues Jahrb. Mineral., Abh*. **176**, 45-66.

Bortnikov, N.S., Mozgova, N.N., Tsepin, A.I. & Breskovska, V.V. (1979): Première expérience de synthèse de chlorosulfosels de Pb/Sb. *Dokl. Akad. Nauk SSSR* **244**, 955-958 (in Russ.).

Breskovska, V.V., Mozgova, N.N., Bortnikov, N.S., Gorshkov, A.I. & Tsepin, A.I. (1982): Ardaite – a new lead–antimony chlorosulphosalt. *Mineral. Mag*. **46**, 357-361.

Bruker, A.X.S. (1998): Saint +, Smart & Xprep Program Package. Bruker Analytical X-ray Systems, Inc., Madison, Wisconsin 53719, USA.

Cervelle, B., Cesbron, F., Sichère, M.-C. & Dietrich, J. (1979): La chalcostibite et la dadsonite de Saint-Pons, Alpes de Haute-Provence, France. *Can. Mineral*. **17**, 601-605.

Ďurovič, S. (1979): Desymmetrization of OD structures. *Kristall und Technik* **14**, 1047-1053.

Franzini, M., Orlandi, P. & Pasero, M. (1992): Morphological, chemical and structural study of robinsonite ($Pb_4Sb_6S_{13}$) from Alpi Apuane, Italy. *Acta Volcanologica* **2**, 231-235.

Jambor, J.L. (1969): Dadsonite (minerals Q and QM), a new lead sulphantimonide. *Mineral. Mag*. **37**, 437-441.

Kostov, V.V. & Macíček, J. (1995): Crystal structure of synthetic $Pb_{12.65}Sb_{11.35}S_{28.35}Cl_{2.65}$ – a new perception of the crystal chemistry of chlorine-bearing lead–antimony sulfosalts. *Eur. J. Mineral*. **7**, 1007-1018.

Léone, P., Le Leuch, L.-M., Palvadeau, P., Molinié, P. & Moëlo, Y. (2003): Single crystal structures and magnetic properties of two iron or manganese–lead–antimony sulfides: $MPb_4Sb_6S_{14}$ (M: Fe, Mn). *Solid State Sci*. **5**, 771-776.

Makovicky, E. (1993): Rod-based sulphosalt structures derived from the SnS and PbS archetypes. *Eur. J. Mineral*. **5**, 545-591.

Makovicky, E. (1997): Modular crystal chemistry of sulphosalts and other complex sulphides. *Eur. Mineral. Union, Notes in Mineralogy* **1**, 237-271.

Makovicky, E. & Balić-Žunić, T. (1998): New measure of distortion for coordination polyhedra. *Acta Crystallogr*. **B54**, 766-773.

MAKOVICKY, E., BALIĆ-ŽUNIĆ, T., KARANOVIĆ, L., POLETI, D. & PRŠEK, J. (2004): Structure refinement of natural robinsonite, $Pb_4Sb_6S_{13}$: cation distribution and modular description. *Neues Jahrb. Mineral., Monatsh.*, 49-67.

MAKOVICKY, E. & MUMME, W.G. (1984): The crystal structures of izoklakeite, dadsonite and jaskolskiite. *15th Int. Congress Crystallogr.* (*Hamburg*), *Coll. Abstr.*, C-246.

MOËLO, Y. (1979): Quaternary compounds in the system Pb–Sb–S–Cl: dadsonite and synthetic phases. *Can. Mineral.* **17**, 595-600.

MOËLO, Y. (1983): Contribution à l'étude des conditions naturelles de formation des sulfures complexes d'antimoine et plomb (sulfosels de Pb/Sb). Signification métallogénique. *Documents du B.R.G.M.* **55**.

MOËLO, Y., BALITSKAYA, O., MOZGOVA, N., SIVTSOV, A. (1989): Chloro-sulfosels de l´indice plombo-antimonifère des Cougnasses (Hautes-Alpes). *Eur. J. Mineral.* **1**, 381-390.

MOËLO, Y., MEERSCHAUT, A., ORLANDI, P. & PALVADEAU, P. (2000) Lead–antimony sulfosalts from Tuscany (Italy). II. Crystal structure of scainiite, $Pb_{14}Sb_{30}S_{54}O_5$, an expanded monoclinic derivative of $Ba_{12}Bi_{24}S_{48}$ hexagonal sub-type (zinkenite group). *Eur. J. Mineral.* **12**, 835-846.

MUMME, W.G. (1989): The crystal structure of $Pb_{5.05}(Sb_{3.75}Bi_{0.28})S_{10.72}Se_{0.28}$: boulangerite of near ideal composition. *Neues Jahrb. Mineral., Monatsh.*, 498-512.

NIIZEKI, W. & BUERGER, M.J. (1957): The crystal structure of jamesonite, $FePb_4Sb_6S_{14}$. *Z. Kristallogr.* **109**, 161-183.

PETROVA, I.V., KUZNETSOV, A.I., BELOKONEVA, E.A. & SIMONOV, M.A. (1978): Crystal structure of boulangerite. *Sov. Phys. Dokl.* **23**, 630-632.

PORTHEINE, J.C. & NOWACKI, W. (1975): Refinement of the crystal structure of zinckenite, $Pb_6Sb_{14}S_{27}$. *Z. Kristallogr.* **141**, 79-96.

SHELDRICK, G.M. (1997a): SHELXS–97. A computer program for crystal structure determination. University of Göttingen, Göttingen, Germany.

SHELDRICK, G.M. (1997b): SHELXL–97. A computer program for crystal structure refinement. University of Göttingen, Göttingen, Germany.

SKOWRON, A. & BROWN, I.D. (1990a): Refinement of the structure of robinsonite, $Pb_4Sb_6S_{13}$. *Acta Crystallogr.* **C46**, 527-531.

SKOWRON, A. & BROWN, I.D. (1990b): Refinement of the structure of boulangerite, $Pb_5Sb_4S_{11}$. *Acta Crystallogr.* **C46**, 531-534.

SRIKRISHNAN, T. & NOWACKI, W. (1974): A redetermination of the crystal structure of cosalite, $Pb_2Bi_2S_5$. *Z. Kristallogr.* **140**, 114-136.

TOPA, D. (2001): *Mineralogy, Crystal Structure and Crystal Chemistry of the Bismuthinite–Aikinite Series from Felbertal, Austria*. Ph.D. thesis, Institute of Mineralogy, University of Salzburg, Austria.

Received January 5, 2006, revised manuscript accepted July 15, 2006.